

Graphene and Poly(3,4-ethylene dioxothiophene):Poly(4-styrenesulfonate) on Nonwoven Fabric as a Room Temperature Metal and Its Application as Dry Electrodes for Electrocardiography

Sneh K. Sinha,[†] Fahad A. Alamer,^{†,‡} Steven J. Woltornist,^{†,§} Yeonsik Noh,^{||} Feiyang Chen,^{†,§} Austin McDannald,[‡] Christopher Allen,^{†,§} Robert Daniels,^{†,§} Ajinkya Deshmukh,[†] Menka Jain,[‡] Ki Chon,^{||} Douglas H. Adamson,^{†,§} and Gregory A. Sotzing^{*,†,§}

[†]Polymer Program, University of Connecticut, 97 North Eagleville Road, Storrs, Connecticut 06269, United States

[‡]Department of Physics, University of Connecticut, 97 North Eagleville Road, Storrs, Connecticut 06269, United States

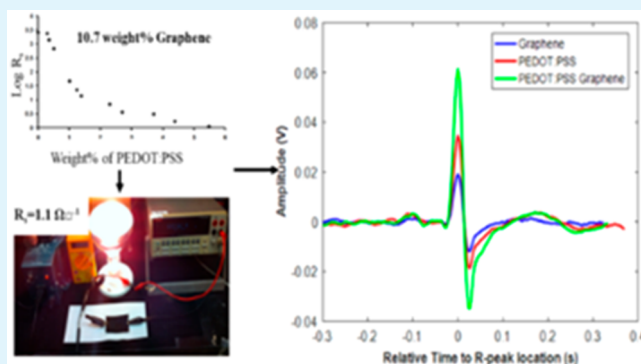
[§]Department of Chemistry, University of Connecticut, 55 North Eagleville Road, Storrs, Connecticut 06269, United States

^{||}Department of Biomedical Engineering, University of Connecticut, 260 Glenbrook Road, Storrs, Connecticut 06269, United States

Supporting Information

ABSTRACT: Highly conductive, metal-like poly(ethylene terephthalate) (PET) nonwoven fabric was prepared by coating poly(3,4-ethylenedioxythiophene):poly(4-styrenesulfonate) (PEDOT:PSS) containing dimethyl sulfoxide (DMSO) onto PET nonwoven fabric previously coated with graphene/graphite. The sheet resistance of the original nonwoven fabric decreases from $>80 \text{ M}\Omega\text{sq}^{-1}$ to $1.1 \text{ }\Omega\text{sq}^{-1}$ after coating with 10.7 wt % graphene and 5.48 wt % PEDOT:PSS with a maximum current at breakdown of 4 A. This sheet resistance is lower than previously reported sheet resistances of fabrics coated with graphene films, PEDOT:PSS films, or PEDOT:PSS coated fabrics from the literature. The effect of temperature on the resistance of graphene/PEDOT:PSS coated fabric has revealed that the resistance decreases with increasing temperature, analogous to semiconductors, with a clear *semiconductor–metal transition* occurring at 290 K. Finally, a coating of 18 wt % graphene/graphite and 2.5 wt % PEDOT:PSS ($R_s = 5.5 \text{ }\Omega\text{sq}^{-1}$) screen printed on the nonwoven fabric was shown to function as an electrode for electrocardiography without any hydrogel and with dry skin conditions. This composite coating finds application in wearable electronics for military and consumer sectors.

KEYWORDS: graphene, PEDOT:PSS, semiconductor–metal transition, wearable electronics



Conductive organic coatings are attracting interest in optoelectronics and functional textiles.^{1,2} Graphene, in particular, has drawn attention due to its outstanding electronic, optical, mechanical, and thermal properties, with its high electrical conductivity attributed to its unique 2D energy dispersion.³ Graphene is a potential solution to one of the major requirements of materials for optoelectronic and photovoltaic devices: finding a replacement for indium tin oxide (ITO) coatings. These coatings need to be optically transparent and exhibit high electrical conductivity and low sheet resistance (R_s). Several groups have studied graphene as an ITO replacement, including Xu and co-workers, who produced graphene films by spin-casting graphene solutions as an electrode for polymer organic photovoltaic cells, reporting sheet resistances as low as $17.9 \text{ K}\Omega\text{sq}^{-1}$ for ca. 25 nm thick graphene.^{4,5} Kymakis and co-workers formed graphene oxide (GO) films by spin-casting on poly(ethylene terephthalate) (PET) substrates and using a laser-based reduction technique

to produce films with a sheet resistance of $0.7 \text{ K}\Omega\text{sq}^{-1}$ for a 20.1 nm thick film.⁶ This value is similar to the sheet resistance of graphene films fabricated by chemically reduced GO films.⁷ Multilayered graphene films on glass or PET substrates using clean-lifting transfer method achieved a sheet resistance of $50 \text{ }\Omega\text{sq}^{-1}$ for nitric acid doped 4-layered graphene films.⁸ Recently, graphene grown by chemical vapor deposition (CVD) was transferred onto tattoo paper for printing graphene devices on the skin. The sheet resistance obtained was ca. $2000 \text{ }\Omega\text{sq}^{-1}$.⁹

Textile based electronic devices are emerging in the field of wearable electronics combining the breathability of the fabric with the functionality of the coated material. Strides have been made in developing graphene coated fabrics over the past few

Received: March 26, 2019

Accepted: August 13, 2019

Published: August 13, 2019

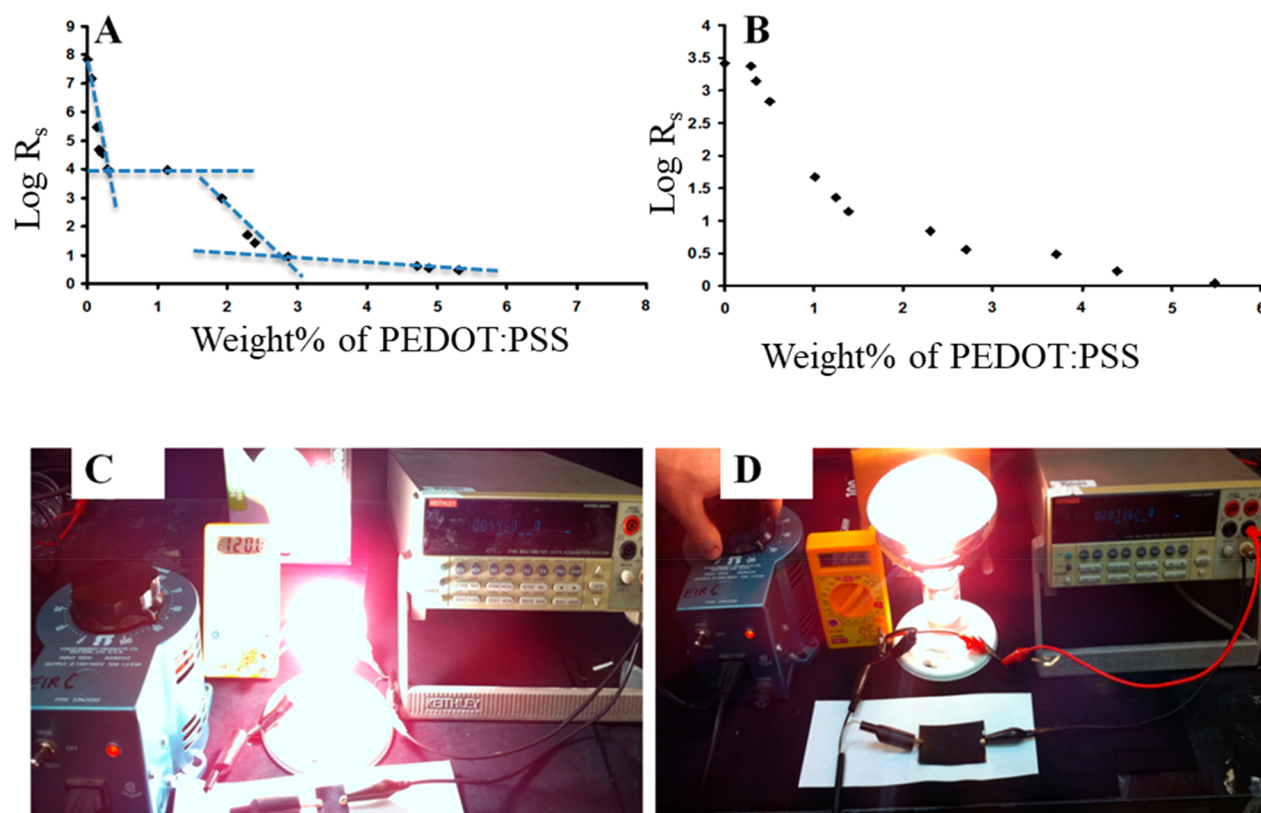


Figure 1. (A, B) Sheet resistance as a function of PEDOT:PSS concentration for fabric containing mixture graphene/graphite at 2.5 and 10.7 wt %, respectively. (C, D) Simple electrical circuit set up to fully light 100 and 250 W light bulbs with a power supply, respectively, using conductive fabric as a simple wire in a series with the power supply and the light bulb; the voltmeter shows the voltage difference between the light bulbs. The sheet resistance of the fabric in (C) and (D) is $1.1 \Omega \square^{-1}$.

years. One method is to soak the fabric with a solution containing graphene oxide (GO), leading to the coating of the fabric with GO and then reducing to reduced graphene oxide (RGO) using sodium hydrosulfite.¹⁰ Other methods reported in the literature produce graphene coated fabric using chemical vapor deposition.¹¹ Molina and co-workers prepared conductive fabric by chemical reduction of GO on polyester fabric and studied the effect of the number of layers coating on the electrical properties with the minimum value of surface resistance being $1.1 \times 10^4 \Omega \square^{-1}$ with three coatings.¹² Though there are various options of incorporating graphene into textiles, sheet resistances obtained are still higher than those of commercially available conducting textile fabrics and ITO coatings on PET.

Conductive polymers (CPs), which consist of alternating single and double bonds, have drawn attention in electronic devices due to their ease of processability, low-cost manufacturing, flexibility, and durability.¹³ Conducting polymers consist of a positively charged polymer backbone with a negatively charged counterion maintaining overall charge neutrality. The water dispersible poly(3,4-ethylene dioxythiophene):poly(styrenesulfonate) (PEDOT:PSS) complex has attracted significant interest among conductive polymers owing to its high transparency, easy aqueous solution processing, high conductivity (when doped), environmental stability, and commercial availability.¹⁴ The addition of chemicals such as dimethyl sulfoxide (DMSO) and ethylene glycol (EG), also known as secondary dopants, has been shown to improve the conductivity of PEDOT:PSS by facilitating phase separation PEDOT chains from insulating

PSS.¹⁵ In the field of smart textiles, conductive fabrics can be prepared by coating the fabric with conductive polymers.¹⁶ The water processability of PEDOT:PSS has also made the open-air coating of PEDOT:PSS possible using inkjet printing, screen printing, and brush printing. Also, hydrophobic coating on the printed PEDOT:PSS coatings has resulted in stability to detergent wash.¹⁷ Otley and co-workers exploited the chemistry of fillers used in textiles such as silica to obtain conducting fabrics with a sheet resistance of $3.2 \Omega \square^{-1}$ with 5.7 wt % PEDOT:PSS.¹⁸ In another study, Alamer fabricated conductive cotton fabric with sheet resistance of $1.58 \Omega \square^{-1}$ using PEDOT:PSS but without using metal or nanoparticles.¹⁹ Besides, open fabrication technique of processing of conducting polymers, vapor phase polymerization of conjugated monomers on textiles has also been developed.²⁰ Vapor phase polymerization of EDOT on fibrous substrates such as paper followed by vapor deposition of a fluorinated polymer film has been shown to have superhydrophobicity and oil repellency.²¹

Recently, a lot of focus has been given by researchers on developing electronic circuitry on skin.²² Such an electronic material has multiple functionalities which include sensors, antennas, and power generation. New materials such as silicon nanomaterials,²² carbon nanomaterials,²³ and liquid metals²⁴ are currently being explored for such applications. One such material is graphene. Graphene has been reported to have high electron mobility of $200\,000 \text{ cm}^2 \text{ V}^{-1} \text{ s}^{-1}$, and graphene coatings have been shown to function as transparent conductors, sensors, and photovoltaic devices.²⁵ In the field of health care, owing to its high surface–volume ratio,

graphene has also been shown to have high signal-to-noise ratio when compared to other dry electrodes such as PDMS/CB for recording electrocardiography (ECG), electromyography (EMG), and electroencephalography (EEG).⁹ Graphene has also been coated onto textiles using chemical vapor deposition or soaking into a graphite solution prepared by Hummer's method.^{26,27} Also, graphene is nontoxic for short to medium term exposure with the skin, an important property for wearable electronics.²⁸ Addition of intrinsically conducting polymers has resulted in lowering of resistances of fibers with graphene serving as interconnects between two chains of conducting polymer.²⁹ Drawing inspiration from the use of hybrid fillers in the conducting transparent electrodes, we have used graphene along with PEDOT:PSS to demonstrate enhanced electronic properties in conducting textiles.

In this paper, we report the fabrication of a hybrid graphite/graphene and PEDOT:PSS fabric by drop-casting and screen printing the aqueous PEDOT:PSS dispersion with incorporated DMSO as a secondary dopant on poly(ethylene terephthalate), PET, nonwoven fabric containing a mixture of pristine graphene and graphite at room temperature. The nonwoven fabric coated in this way shows low sheet resistance, $1.1 \Omega \square^{-1}$, with a maximum current of 4 A at breakdown. The effect of temperature on the system's resistance, over the range of 10–400 K, revealed a clear semiconductor–metallic transition at room temperature. The composite textile has also been shown to function as dry electrodes for electrocardiography with PEDOT:PSS serving as an electrical adhesive for graphene/graphite coatings.

Investigating the effect of PEDOT:PSS on the sheet resistance used fabrics containing different concentrations of graphene coating. We focused our attention on the fabric containing low and high graphene/graphite concentrations. The measurements were carried out using a four-line probe technique for $2.5 \times 2.5 \text{ cm}^2$ samples. As shown in Figure 1, the sheet resistance of the fabric containing graphene/graphite decreases by increasing the concentration of PEDOT:PSS. At low graphene/graphite concentrations, 2.5 wt %, the influence of the PEDOT:PSS on the sheet resistance of the fabric was clear, Figure 1A, with a drop of 6 orders of magnitude, from $77.9 \text{ M } \Omega \square^{-1}$ for fabric treated with graphene/graphite to $51.3 \Omega \square^{-1}$ for the sample treated with 2.29 wt % PEDOT:PSS. We set this concentration as the percolation threshold, since increasing the concentration above these values did not drop the sheet resistance by an order of magnitude. For fabric infused with high graphene/graphite concentrations, 10.7 wt %, the sheet resistance only dropped by 1 order of magnitude. We also see a distinct two-step percolation when the initial graphene loading is 2.5 wt % (Figure 1A), although the effect is not pronounced for fabric treated with 10.7 wt % graphene/graphite (Figure 1B). The resistance of the samples reached a minimum value of $1.1 \Omega \square^{-1}$ with the maximum current at breakdown reaching 4 A. Table S1 (Supporting Information S1) summarizes the lowest sheet resistances obtained from different combinations of graphene/graphite while maintaining the concentration of PEDOT:PSS constant.

To confirm passage of high current in the fabric containing the hybrid containing 10.6 wt % graphene/graphite and 5.7 wt % PEDOT:PSS ($R_s = 1.1 \Omega \square^{-1}$), an electrical circuit was constructed as shown in Figure 1C. We connected a 100 W light bulb in series with the hybrid fabric, and an AC 0.854 A current was applied across the fabric. Powering the light to full

intensity showed no visible evidence of sample breakdown. In another application, connecting a 250 W heat lamp (Figure 1D) in series with the fabric ($3.75 \times 6.25 \text{ cm}^2$) and applying an AC 2.87 A current across the fabric and the light at full intensity showed no evidence of sample breakdown.

To understand the mechanism responsible for the decrease in the sheet resistance of the hybrid conductor system, we studied the effect of temperature on the resistance of the fabric over the temperature range of 10–400 K. First, we investigated the effect of temperature on the resistance of the fabric containing a 6.20 and 14.74 wt % graphene/graphite mixture. Figure S1 (Supporting Information S2) shows the decrease in resistance with an increase in temperature up to 350 K which is consistent with semiconducting behavior resulting from the disorder of the graphene/graphite sheet structure at low temperature where electron localization and hopping play a significant role. In the range of 100–250 K, the resistance is relatively constant, being 1 M Ω for 6.2 wt % and 5 K Ω for 14.74 wt % graphene/graphite. At 350 K, the conductive fabric undergoes a distinct insulator–metal transition, indicating a modulation of the band gap. Next, we investigated the effect of temperature on the resistance of the infused fabric containing 14.7 wt % graphene/graphite treated with 0.58 wt % PEDOT:PSS (Figure 2) over a wide temperature range (10–

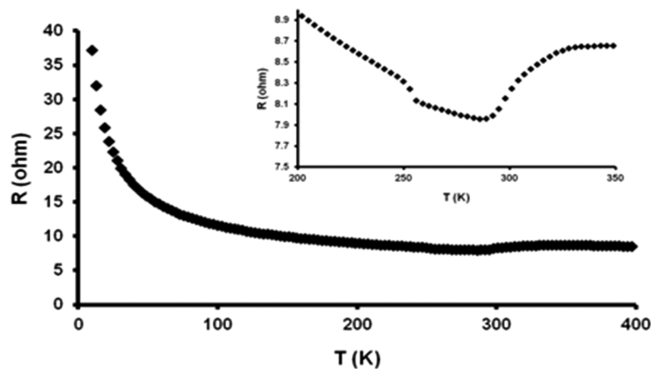


Figure 2. Resistance vs temperature $R(T)$ values for PET conducting fabric containing 14.7 wt % graphene/graphite and 0.58 wt % PEDOT:PSS. The inset shows the semiconductor–insulator transition.

400 K). The sample had an area of $10 \times 5 \text{ mm}^2$ with a resistance of ca. 15Ω , and the measurements were carried out using a standard four-point probe from Physical Property Measurement System (Quantum Design). As shown in Figure 2, the resistance exhibited semiconducting behavior up to 200 K, with a relatively constant resistance value from 200 to 400 K. Upon close inspection, a clear semiconductor-metal transition occurs at 290 K (inset Figure 2) due to the incorporation of graphene. The charge transport of the hybrid conductor occurs because of tunneling and hopping conduction, with the mobility given by the equation:

$$\mu = \mu_{\text{hop}} + \mu_{\text{tun}} \quad (1)$$

where μ_{hop} and μ_{tun} are given by the equations:

$$\mu_{\text{hop}} = \frac{e^2 a^2 t^2}{k_B T \hbar^2 \omega_0} \left[\frac{\pi}{g^2 \text{csch}\left(\frac{\hbar \omega_0}{2k_B T}\right)} \right]^{1/2} \exp\left[-2g^2 \tanh\left(\frac{\hbar \omega_0}{4k_B T}\right)\right] \quad (2)$$

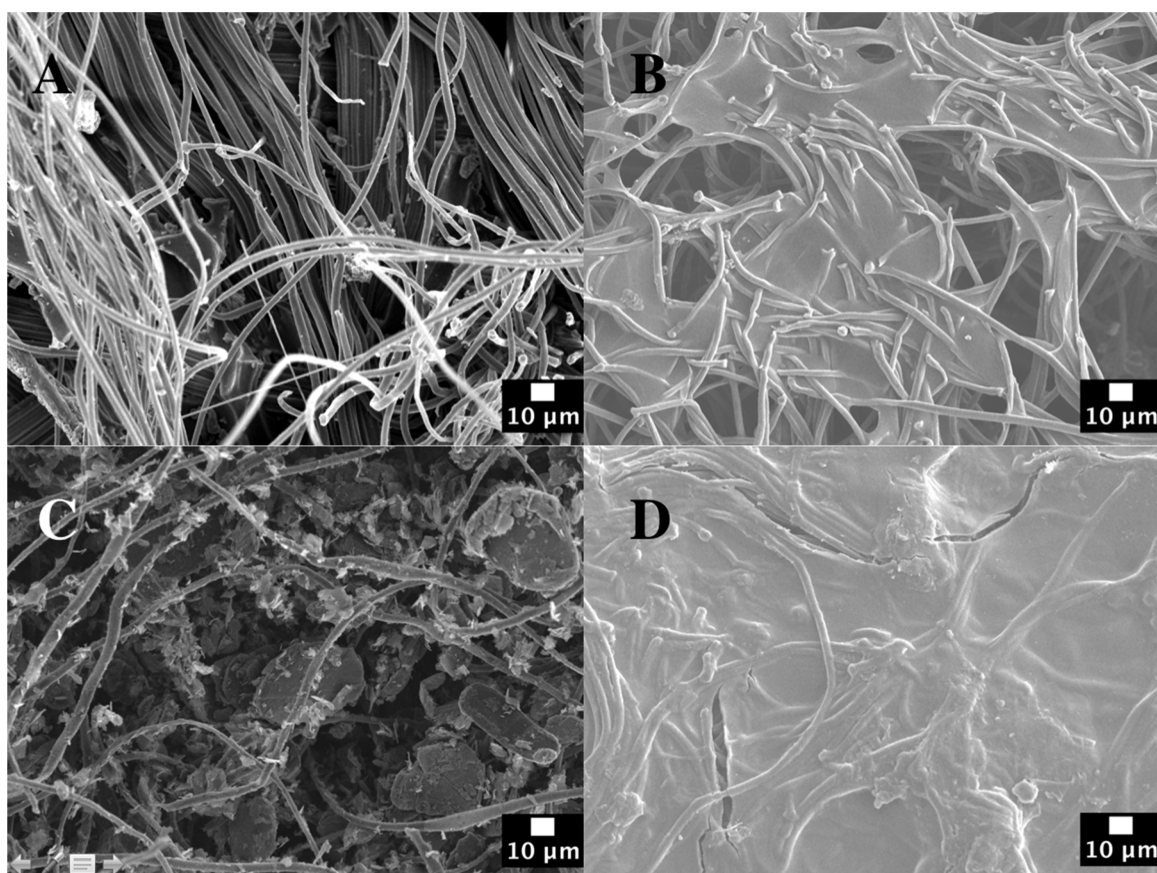


Figure 3. Scanning electron microscopy images for (A) untreated fabric, (B) fabric treated with 0.58 wt % PEDOT:PSS, (C) fabric treated with the 14.7 wt % graphene/graphite, and (D) fabric treated with the hybrid 10.7 wt % graphene/graphite and 5.48 wt % PEDOT:PSS.

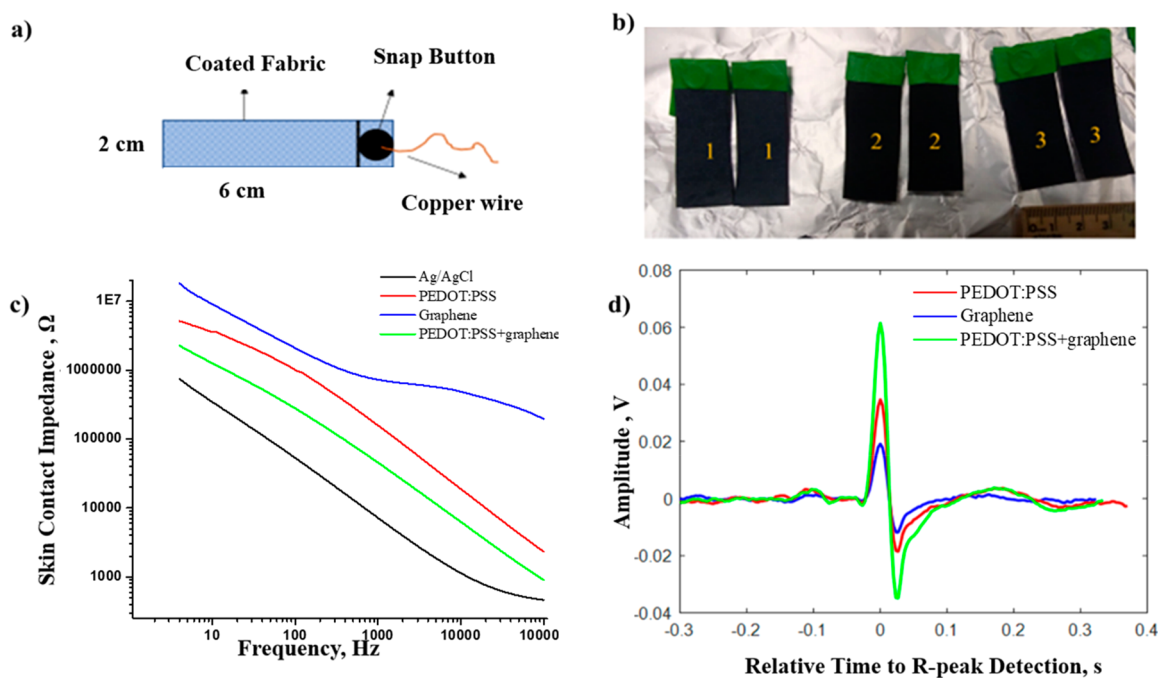


Figure 4. Fabrication of ECG electrodes. (a) Dimensions of printed electrodes for ECG. (b) Image of different electrodes: (1) PEDOT:PSS, (2) graphene, and (3) graphene and PEDOT:PSS. (c) Skin contact impedance of electrodes at rest: graphene (blue); PEDOT:PSS (red); PEDOT:PSS + graphene (green); Ag/AgCl (black). (d) Electrocardiogram signal obtained from different electrodes: graphene (blue); PEDOT:PSS (red); PEDOT:PSS + graphene (green).

$$\mu_{\text{tun}} = \frac{e^2 a^2 w_0}{k_B T} \left[\frac{g^2 \operatorname{csch}\left(\frac{\hbar\omega_0}{2k_B T}\right)}{\pi} \right]^{1/2} \exp\left[-2g^2 \operatorname{csch}\left(\frac{\hbar\omega_0}{2k_B T}\right)\right] \quad (3)$$

where e is the electron charge, $\hbar\omega_0$ is the phonon energy, t is the transfer integral, k_B is Boltzmann's constant, and g is a coupling constant.³⁰ The incorporation of graphene into the PEDOT:PSS leads to enhanced tunneling conduction at low temperatures and hopping conduction at high temperatures. This is because graphene doping leads to an increase in the space between the PEDOT chains resulting in an increase in the diffusion coefficient of the charge carriers which increases μ_{hop} and μ_{tun} according to the Einstein–Smoluchowski equation:

$$\mu = \frac{eD}{k_B T} \quad (4)$$

where e is the electron charge, D is the diffusion coefficient, k_B is Boltzmann's constant, and T is the temperature. We hypothesize that that graphene doping PEDOT:PSS decreases the disorder strength leading to an increase in charge mobility and thus a decrease in resistance.³⁰

The morphology of the system was determined using a field emission scanning electron microscope (JEOL 6335 FESEM). Figure 3A illustrates the fabric before treatment with slight bundling of the individual fibers observed. The images taken of the fabric coated with PEDOT:PSS seem to suggest that the coating is primarily on the surface of the fabric, as the surface tension of the fluid holds it between the fibers (Figure 3B). There is, however, still some fluid that penetrates deeper into the sample. In Figure 3C, the fabric only treated with the graphene/graphite mixture is shown. These images show the fabric's fibers coated with graphene with some bulk graphite caught between the fibers. The amount of graphite in the sample is assumed to decrease closer to the middle. The final image, Figure 3D, shows the fabric with the combination of PEDOT:PSS and graphene/graphite. Since the coating with PEDOT:PSS is performed after the infusion of graphene/graphite, PEDOT:PSS seals the coated graphene/graphite, and some particles of graphene/graphite are apparent under the wrinkles in the PEDOT:PSS coating.

The treated fabric ($R_s = 1.1 \Omega \square^{-1}$) was also tested against a control PET nonwoven fabric in an Instron Model 1011 for tensile strength. There was a ca. 45% increase in tensile strength of the treated fabric when compared to the control (Figure S2, Supporting Information S3). Looking at the scanning electron microscope images, one can see that the conductive polymer connects the fibers of the fabric. This bridging can be thought to be the source of the increased strength.

To demonstrate the current carrying capacities of graphene electrodes, we tested graphene-coated textile as an electrocardiogram electrode with dimensions of 2 cm \times 6 cm (Figure 4a and b). One subject was recruited to check the efficacy of the fabricated electrode, 18 wt % graphene coated textile electrode, showed a skin contact impedance in the order of $10^7 \Omega$ at 10 Hz which is approximately 2 orders of magnitude higher than that of Ag/AgCl (Figure 4c). Next, we recorded the electrocardiogram signal with Ag/AgCl as a benchmark electrode. The amplitude of the ECG signal obtained was 30 mV with a signal-to-noise ratio of approximately 16.5 dB in dry

skin conditions. Yapici and co-workers have reported the response of an ECG electrode made from graphene coated textile from the wrist and found it to be at par with commercially available Ag/AgCl.³¹ The signal amplitude from this study showed a substantially lower amplitude than that of Ag/AgCl electrodes, most likely as a result of high skin contact impedance compared to Ag/AgCl electrodes. The other problem from graphene coated textile is leaching of graphene onto the skin during the ECG measurements. To solve the problem of graphene rubbing onto the skin during ECG measurement, we coated PEDOT:PSS onto a graphene-coated textile. PEDOT:PSS has been used in the past for the fabrication of biopotential electrodes because of its mixed nature of conduction.³² Three layers of PEDOT:PSS ink containing DMSO was screen printed sequentially onto graphene coated textile which corresponds to 2.5 wt % PEDOT:PSS ($R_s = 5.5 \Omega/\square$). The skin contact impedance from the PEDOT:PSS electrode and PEDOT:PSS–graphene coated electrode is shown in Figure 4c with the composite electrode showing lower impedance than the either PEDOT:PSS or graphene electrode. The ECG signal obtained from the mixed conductor electrode showed an increase in amplitude and signal-to-noise compared with individual electrodes (Table S2, Supporting Information S4) The ECG trace obtained from the three electrodes is shown in Figure 4d with mixed conductor electrodes showing the highest amplitude. The reason behind this increase is most likely due to an increase in the number of charge carrying groups as a result of the addition of graphene coating making the flow of ionic current from the body to the electrode much better. Additionally, the PEDOT:PSS coating on the graphene coated textile served as an “electrical adhesive” preventing graphene from being leached onto the skin.

In summary, we prepared a highly conductive, metallic behaving fabric using a mixture of graphene/graphite and PEDOT:PSS. The lowest sheet resistance achieved was $1.1 \Omega/\square$ which is the lowest value reported for hybrid PEDOT:PSS and graphene/graphite conductor. We attribute this low sheet resistance to PEDOT:PSS acting as the primary dopant. Resistance versus temperature profile indicates the semiconductor to metal transition at 300 K. Finally, to demonstrate the practical usage, a 250 W lamp was illuminated using conducting PET fabric as a wire. The hybrid conductor comprising PEDOT:PSS and graphene/graphite has been shown to function as a biopotential electrode in dry skin conditions without the need of hydrogel.

EXPERIMENTAL SECTION

Materials. PEDOT:PSS dispersion (Clevios PH1000) was procured from Heraeus. Dimethyl sulfoxide (DMSO) was purchased from Sigma-Aldrich and used as received. Nike, Inc. provided the PET nonwoven fabric, graphite was provided by Asbury Carbons (Grade 3243), and *n*-heptane was obtained from Fisher Scientific, 99% Optima. Ag/AgCl chloride was obtained from ConMed Corporation, U.S.A. A Speedball screen printing setup was obtained from Jo-Ann Fabrics.

Sample Preparation. The fabrication of the high conductivity nonwoven fabric was based on two steps. In the first step, the graphite/graphene coated fabric is fabricated using an interfacial trapping method.^{29,33} Exfoliation of the graphite was accomplished by using a mixture containing 5 mL of heptane and 100 mg of graphite, tip sonication for 30 min, then the addition of 5 mL of water, followed by bath sonication for an additional 30 min as per the procedure reported by Woltornist and co-workers.²⁹ The mixture was

then added to a vial containing a swatch of nonwoven PET fabric, $2.5 \times 2.5 \text{ cm}^2$ and bath sonicated for 1 h, after which the fabric sample was removed and dried. In the second step, the dried graphite/graphene coated fabric was treated with PEDOT:PSS with 5% DMSO by drop casting until saturation. The fabric was air-dried for 30 min and then dried in an oven at $110 \text{ }^\circ\text{C}$ for 1 h to remove water. The concentration of PEDOT:PSS in the fabric was calculated as the difference in weight between the fabric before and after adding PEDOT:PSS. Repetitive drop casting/drying cycles referred to as “dipping cycles”, increased the PEDOT:PSS concentration in the fabric. PEDOT:PSS ink was made from a formulation containing 95% Clevious PH 1000 and 5% DMSO and concentrated to 40% of its original weight by evaporating water at $60 \text{ }^\circ\text{C}$ for 6 h. Screen printing was carried out using a Speedball screen with a nylon mesh of mesh count 110, and the squeegee was held at 45° using a custom-made holder. The printing speed was approximately 50 mm/s.

Protocol for ECG Measurement. One male subject was recruited for this study. Oral consent was obtained from the subject. An ECG monitoring device was fabricated for measuring single lead ECG signals. Each ECG circuit obtained a Lead I signal from the chest via two electrodes with a virtual right-leg driven circuit. This single lead ECG device used for screen printed PEDOT:PSS electrodes provided a 3 dB cutoff from 0.5 to 150 Hz with the use of a second-order band-pass filter and a sampling rate of 300 Hz. The filtered analog ECG signals were converted to digital data by using a 12 bit analog-to-digital converter (ADC) embedded in a microcontroller (MSP430F2618, Texas Instruments). A six-point moving average notch filter was applied to the ECG signals for 60 Hz power noise rejection. The ECG signals were transmitted to a personal computer via Bluetooth wireless communication. A LabVIEW software (National Instruments) graphic user interface software was developed for real-time display and data storage for further off-line data analysis. Ag/AgCl snap buttons were used to connect leads to the ECG device, and an elastic chest strap was used to immobilize the electrodes onto the subject's chest. For fabric-based electrodes, a chest strap was placed with one electrode on the left and the other electrode on the right side of the rib cage. Each experiment lasted 1 min in the sitting position and subjects were instructed to remain relaxed during each experiment. A 30 s ECG segment containing stable data was chosen for analysis. First, the acquired ECG data was filtered with a fourth-order Butterworth band-pass filter with the cutoff bandwidth between 0.1 and 40 Hz. A nonlocal mean filtering algorithm as a secondary filtering step was applied offline to minimize the high-frequency noise observed in the collected data.

Signal Processing. After filtering, R-wave peak detection was performed on the selected ECG segments using a robust QRS complex detection algorithm. ECG templates were computed for each selected ECG segment by creating an ensemble matrix with the corresponding ECG cycles aligned with respect to their R-peak locations and then averaged at each time instant. ECG amplitude was calculated using peak-to-peak values in each ECG template. The amplitude of the ECG signal from the fabric electrodes was then compared to commercially available Ag/AgCl.

Sample Characterization. The resistance measurements were carried out using four-line probes and the sheet resistance calculated from the equation $R_s = R(w/l)$ where R is the resistance which was calculated from an I - V curve, w is the width of the sample (2.5 cm), and l is the distance between the leads (0.35 cm). A Power Supply 3630 was used to apply current, while a 196 system DMA was used to measure the voltage. A variable transform was used in the fabric electrical circuit. Electron microscopy was performed using an AMRAY 1810 scanning electron microscope. Resistance values were measured as a function of temperature (from 10 to 400 K) using a standard four-probe technique in a physical property measurement system (Quantum Design).

■ ASSOCIATED CONTENT

📄 Supporting Information

The Supporting Information is available free of charge on the ACS Publications website at DOI: [10.1021/acsami.9b05379](https://doi.org/10.1021/acsami.9b05379).

Minimum sheet resistance of microfibers versus amount of hybrid conductor; resistance vs temperature graph of graphene/graphite coated textiles; stress–strain graph of coated fabrics; signal-to-noise ratio and amplitude of textile coated electrodes (PDF)

■ AUTHOR INFORMATION

Corresponding Author

*E-mail: g.sotzing@uconn.edu. Telephone: 860-486-4619.

ORCID

Sneh K. Sinha: 0000-0003-0555-0282

Douglas H. Adamson: 0000-0002-7719-9287

Notes

The authors declare no competing financial interest.

■ REFERENCES

- (1) Berggren, M.; Nilsson, D.; Robinson, N. D. Organic Materials for Printed Electronics. *Nat. Mater.* **2007**, *6* (1), 3–5.
- (2) Takamatsu, S.; Lonjaret, T.; Crisp, D.; Badier, J.-M.; Malliaras, G. G.; Ismailova, E. Direct Patterning of Organic Conductors on Knitted Textiles for Long-Term Electrocardiography. *Sci. Rep.* **2015**, *5*, 15003.
- (3) Allen, M. J.; Tung, V. C.; Kaner, R. B. Honeycomb Carbon: A Review of Graphene. *Chem. Rev.* **2010**, *110* (1), 132–145.
- (4) Inganäs, O. Organic Photovoltaics: Avoiding Indium. *Nat. Photonics* **2011**, *5* (4), 201–202.
- (5) Xu, Y.; Long, G.; Huang, L.; Huang, Y.; Wan, X.; Ma, Y.; Chen, Y. Polymer Photovoltaic Devices with Transparent Graphene Electrodes Produced by Spin-Casting. *Carbon* **2010**, *48* (11), 3308–3311.
- (6) Kymakis, E.; Savva, K.; Stylianakis, M. M.; Fotakis, C.; Stratakis, E. Flexible Organic Photovoltaic Cells with In Situ Nonthermal Photoreduction of Spin-Coated Graphene Oxide Electrodes. *Adv. Funct. Mater.* **2013**, *23* (21), 2742–2749.
- (7) Yin, Z.; Sun, S.; Salim, T.; Wu, S.; Huang, X.; He, Q.; Lam, Y. M.; Zhang, H. Organic Photovoltaic Devices Using Highly Flexible Reduced Graphene Oxide Films as Transparent Electrodes. *ACS Nano* **2010**, *4* (9), 5263–5268.
- (8) Wang, D.-Y.; Huang, I.-S.; Ho, P.-H.; Li, S.-S.; Yeh, Y.-C.; Wang, D.-W.; Chen, W.-L.; Lee, Y.-Y.; Chang, Y.-M.; Chen, C.-C.; et al. Clean-Lifting Transfer of Large-Area Residual-Free Graphene Films. *Adv. Mater.* **2013**, *25* (32), 4521–4526.
- (9) Kabiri Ameri, S.; Ho, R.; Jang, H.; Tao, L.; Wang, Y.; Wang, L.; Schnyer, D. M.; Akinwande, D.; Lu, N. Graphene Electronic Tattoo Sensors. *ACS Nano* **2017**, *11* (8), 7634–7641.
- (10) Fugetsu, B.; Sano, E.; Yu, H.; Mori, K.; Tanaka, T. Graphene Oxide as Dyestuffs for the Creation of Electrically Conductive Fabrics. *Carbon* **2010**, *48* (12), 3340–3345.
- (11) Li, X.; Sun, P.; Fan, L.; Zhu, M.; Wang, K.; Zhong, M.; Wei, J.; Wu, D.; Cheng, Y.; Zhu, H. Multifunctional Graphene Woven Fabrics. *Sci. Rep.* **2012**, *2* (1), 395.
- (12) Molina, J.; Fernández, J.; Inés, J. C.; del Río, A. I.; Bonastre, J.; Cases, F. Electrochemical Characterization of Reduced Graphene Oxide-Coated Polyester Fabrics. *Electrochim. Acta* **2013**, *93*, 44–52.
- (13) MacDiarmid, A. G.; Min, Y.; Wiesinger, J. M.; Oh, E. J.; Scherr, E. M.; Epstein, A. J. Towards Optimization of Electrical and Mechanical Properties of Polyaniline: Is Crosslinking between Chains the Key? *Synth. Met.* **1993**, *55* (2–3), 753–760.
- (14) Sotzing, G. A.; Briglin, S. M.; Grubbs, R. H.; Lewis, N. S. Preparation and Properties of Vapor Detector Arrays Formed from

Poly(3,4-Ethylenedioxy)Thiophene-Poly(Styrene Sulfonate)/Insulating Polymer Composites. *Anal. Chem.* **2000**, *72* (14), 3181–3190.

(15) Palumbini, C. M.; Heller, C.; Schaffer, C. J.; Körstgens, V.; Santoro, G.; Roth, S. V.; Müller-Buschbaum, P. Molecular Reorientation and Structural Changes in Cosolvent-Treated Highly Conductive PEDOT:PSS Electrodes for Flexible Indium Tin Oxide-Free Organic Electronics. *J. Phys. Chem. C* **2014**, *118* (25), 13598–13606.

(16) Ding, Y.; Invernale, M. A.; Sotzing, G. A. Conductivity Trends of PEDOT-PSS Impregnated Fabric and the Effect of Conductivity on Electrochromic Textile. *ACS Appl. Mater. Interfaces* **2010**, *2* (6), 1588–1593.

(17) Guo, Y.; Otle, M. T.; Li, M.; Zhang, X.; Sinha, S. K.; Treich, G. M.; Sotzing, G. A. PEDOT:PSS “Wires” Printed on Textile for Wearable Electronics. *ACS Appl. Mater. Interfaces* **2016**, *8* (40), 26998–27005.

(18) Otle, M. T.; Alamer, F. A.; Guo, Y.; Santana, J.; Eren, E.; Li, M.; Lombardi, J.; Sotzing, G. A. Phase Segregation of PEDOT:PSS on Textile to Produce Materials of $> 10 \text{ A Mm}^{-2}$ Current Carrying Capacity. *Macromol. Mater. Eng.* **2017**, *302* (3), 1600348.

(19) Alhashmi Alamer, F. A Simple Method for Fabricating Highly Electrically Conductive Cotton Fabric without Metals or Nanoparticles, Using PEDOT:PSS. *J. Alloys Compd.* **2017**, *702*, 266–273.

(20) Zhang, L.; Fairbanks, M.; Andrew, T. L. Rugged Textile Electrodes for Wearable Devices Obtained by Vapor Coating Off-the-Shelf, Plain-Woven Fabrics. *Adv. Funct. Mater.* **2017**, *27* (24), 1700415.

(21) Im, S. G.; Kusters, D.; Choi, W.; Baxamusa, S. H.; van de Sanden, M. C. M.; Gleason, K. K. Conformal Coverage of Poly(3,4-Ethylenedioxythiophene) Films with Tunable Nanoporosity via Oxidative Chemical Vapor Deposition. *ACS Nano* **2008**, *2* (9), 1959–1967.

(22) Kim, D.-H.; Lu, N.; Ma, R.; Kim, Y.-S.; Kim, R.-H.; Wang, S.; Wu, J.; Won, S. M.; Tao, H.; Islam, A.; et al. Epidermal Electronics. *Science* **2011**, *333* (6044), 838–843.

(23) Lee, S. M.; Byeon, H. J.; Lee, J. H.; Baek, D. H.; Lee, K. H.; Hong, J. S.; Lee, S.-H. Self-Adhesive Epidermal Carbon Nanotube Electronics for Tether-Free Long-Term Continuous Recording of Biosignals. *Sci. Rep.* **2015**, *4* (1), 6074.

(24) Kuo, P.-H.; Tzeng, T.-H.; Huang, Y.-C.; Chen, Y.-H.; Chang, Y.-C.; Ho, Y.-L.; Wu, J.-T.; Lee, H.-H.; Lai, P.-J.; Liu, K.-Y.; et al. Non-Invasive Drosophila Ecg Recording by Using Eutectic Gallium-Indium Alloy Electrode: A Feasible Tool for Future Research on the Molecular Mechanisms Involved in Cardiac Arrhythmia. *PLoS One* **2014**, *9* (9), No. e104543.

(25) Bae, S.; Kim, H.; Lee, Y.; Xu, X.; Park, J.-S.; Zheng, Y.; Balakrishnan, J.; Lei, T.; Ri Kim, H.; Song, Y. I.; et al. Roll-to-Roll Production of 30-Inch Graphene Films for Transparent Electrodes. *Nat. Nanotechnol.* **2010**, *5* (8), 574–578.

(26) Neves, A. I. S.; Bointon, T. H.; Melo, L. V.; Russo, S.; de Schrijver, I.; Craciun, M. F.; Alves, H. Transparent Conductive Graphene Textile Fibers. *Sci. Rep.* **2015**, *5* (1), 9866.

(27) Yapici, M.; Alkhidir, T. Intelligent Medical Garments with Graphene-Functionalized Smart-Cloth ECG Sensors. *Sensors* **2017**, *17* (4), 875.

(28) Pelin, M.; Fusco, L.; León, V.; Martín, C.; Criado, A.; Sosa, S.; Vázquez, E.; Tubaro, A.; Prato, M. Differential Cytotoxic Effects of Graphene and Graphene Oxide on Skin Keratinocytes. *Sci. Rep.* **2017**, *7*, 40572.

(29) Woltornist, S. J.; Alamer, F. A.; McDannald, A.; Jain, M.; Sotzing, G. A.; Adamson, D. H. Preparation of Conductive Graphene/Graphite Infused Fabrics Using an Interface Trapping Method. *Carbon* **2015**, *81*, 38–42.

(30) Coropceanu, V.; Cornil, J.; da Silva Filho, D. A.; Olivier, Y.; Silbey, R.; Brédas, J.-L. Charge Transport in Organic Semiconductors. *Chem. Rev.* **2007**, *107* (4), 926–952.

(31) Yapici, M. K.; Alkhidir, T.; Samad, Y. A.; Liao, K. Graphene-Clad Textile Electrodes for Electrocardiogram Monitoring. *Sens. Actuators, B* **2015**, *221*, 1469–1474.

(32) Sinha, S. K.; Noh, Y.; Reljin, N.; Treich, G. M.; Hajeb-Mohammadalipour, S.; Guo, Y.; Chon, K. H.; Sotzing, G. A. Screen-Printed PEDOT:PSS Electrodes on Commercial Finished Textiles for Electrocardiography. *ACS Appl. Mater. Interfaces* **2017**, *9*, 37524.

(33) Woltornist, S. J.; Oyer, A. J.; Carrillo, J.-M. Y.; Dobrynin, A. V.; Adamson, D. H. Conductive Thin Films of Pristine Graphene by Solvent Interface Trapping. *ACS Nano* **2013**, *7* (8), 7062–7066.